Original Article

Characteristic differences of cell sheets composed of mesenchymal stem cells with different tissue origins

Mitsuyoshi Nakao, Daimu Inanaga, Kenichi Nagase*, Hideko Kanazawa**

Faculty of Pharmacy, Keio University, 1-5-30 Shibakoen, Minato, Tokyo, 105-8512, Japan

ABSTRACT

Introduction: Stem cell therapy with mesenchymal stem cells (MSCs) has been widely used in many clinical trials, and therapy with MSC sheets shows promise for patients. However, there are few reports characterizing MSC sheets. In the present study, the properties of MSC sheets derived from bone marrow, adipose tissue, and umbilical cord were evaluated.
Methods: Cell sheets were fabricated with MSCs from different tissue origins in temperature-responsive cell culture dishes with and without pre-coating of fetal bovine serum (FBS). MSC adhesion behavior in the culture dish was observed. Secretion of cytokines related to cell proliferation and immune regulation from MSC sheets was investigated by ELISA. The adhesion properties of the MSC sheets were investigated by time-lapse microscopy.
Results: Different cell adhesion and proliferation rates in temperature-responsive cell culture dishes were observed among the three types of MSCs. FBS pre-coating of the dishes enhanced cell attachment and proliferation in all cell types. Harvested cell sheets showed high attachment capacity to tissue culture polystyrene dish surfaces.
Conclusions: MSC sheets can be fabricated from MSCs from different tissue origins using temperature-responsive cell culture dishes. The fabricated MSC sheets could be useful in cell transplantation therapies by choosing appropriate types of MSCs that secrete therapeutic cytokines for the targeted diseases.
© 2019, The Japanese Society for Regenerative Medicine. Production and hosting by Elsevier B.V. This is an open access article under the CC BY-NC-ND license (http://creativecommons.org/licenses/by-nc-nd/4.0/).

1. Introduction

Recently, mesenchymal stem cell (MSC) products have been approved for the purpose of cell therapy worldwide, and great expectation has been placed on their therapeutic effect [1]. MSCs have the ability to self-proliferate and show multipotency to differentiate into various cell types such as adipose, nerve, bone, and cartilage cells [2]. MSCs can be collected from several tissues and are frequently isolated from umbilical cord, bone marrow, and adipose tissue because of their high proliferation ability and easily accessible cell sources [3]. In MSC therapy, the paracrine effect is considered the main underlying mechanism [4,5]. In the effect, MSCs secrete soluble factors (cytokines) at the injured site and mediate therapeutic effects such as anti-inflammatory, anti-fibrotic, and anti-apoptotic effects. MSCs also transdifferentiate and regenerate to directly repair the injured site. Also, the effect of MSCs involves secretion of soluble factors (cytokines) into vessels and homing to distant injured tissues. To achieve the effect, cells are required to survive in the long term. MSCs are known to enhance angiogenesis and suppress immune systems through secretion of cytokines. Angiogenesis is mediated by growth factors (e.g., vascular endothelial growth factor (VEGF), hepatocyte growth factor (HGF)) and immune suppression is mediated by the secretion of prostaglandin E2 (PGE_2), transforming growth factor (TGF)-β, and interleukins (ILs; e.g., IL-6, IL-10) [4—6].

On the contrary, to improve cell transplantation therapy, various cell transplantation methods have been investigated [7,8]. In most cases, cell transplantation was performed by direct injection into the affected area. However, the injected cells were not effectively transplanted because they did not survive in the host

* Corresponding author. Fax: +81 03 5400 1378.
** Corresponding author.
 E-mail addresses: nagase-kn@pha.keio.ac.jp (K. Nagase), kanazawa-hd@pha.keio.ac.jp (H. Kanazawa).

tissue [9]. To overcome this issue, cell transplantation using cell sheets was developed. These cell sheets are fabricated using unique cell culture dishes modified with thin grafted layers of a temperature-responsive polymer, poly(N-isopropylacrylamide) (PNIPAAm) [10–15]. PNIPAAm is well-known to have an aqueous lower critical solution temperature of 32 °C, close to body temperature [16]. Thus, the polymer has been widely utilized in biomedical applications, including drug delivery [17–20], biosensors and imaging agents [21–24], bioseparations [25–30], and temperature-responsive cell culture dishes [10–15,31–34]. Temperature-responsive cell culture dishes change rapidly from hydrophobic to hydrophilic as the aqueous temperature is reduced below 32 °C. Using this approach, adherent cells cultured on temperature-responsive cell culture dishes can be harvested without any enzyme treatment as a contiguous intact viable cell sheet. Aqueous medium spontaneously penetrates into the PNIPAAm polymer interface between the adherent cells and the temperature-responsive cell culture dish surface at temperatures below 32 °C, thus expanding the PNIPAAm chains by hydration and physically separating the cell surfaces from the temperature-responsive cell culture dish surface [10,35,36]. This cell sheet technology represents a unique method for gentle and non-destructive harvesting of cells, thereby enabling adherent cells to be harvested from temperature-responsive cell culture dishes with maintained cell activity and no destruction of the extracellular matrix (ECM) [37–39].

Thus, cell sheets can be easily transplanted into patients without sutures because the ECM proteins remaining in the cell sheets act as a tissue-adhesive glue. Using these properties, various types of cell sheets have been applied to tissue engineering and regenerative medicine [40–54]. Among these approaches, therapy with MSC sheets shows promise because of the therapeutic effect of MSCs described above. However, there are few reports on the characterization of MSC sheets, and the cell sheet properties require further investigation for improved transplantation. In addition, MSCs can be obtained from various tissues, including bone marrow, adipose tissue, and umbilical cord. The differences in properties of the resulting MSC sheets require clarification.

In the present study, the properties of MSC sheets derived from umbilical cord, bone marrow, and adipose tissue were evaluated. Specifically, cell adhesion and proliferation on temperature-responsive cell culture dishes were investigated, and cytokine secretion from MSC sheets was measured. The attachment behavior of the MSC sheets was also observed.

2. Materials and methods

2.1. Cell culture

Human MSCs derived from umbilical cord (UC-MSCs) and bone marrow (BM-MSCs) were obtained from PromoCell (Heidelberg, Germany). Human adipose tissue-derived MSCs (AD-MSCs) were obtained from Lonza (Basel, Switzerland). All cells were cultured in standard culture medium comprising Dulbecco's modified Eagle's medium (DMEM) (Gibco, Rockville, MD, USA) supplemented with 10% fetal bovine serum (FBS) (BIOSERA, Ringmer, UK), 1% GlutaMAX (Gibco), 1% MEM non-essential amino acids (Gibco), 100 U/mL penicillin, and 100 μg/mL streptomycin (Gibco). The cells were cultured at 37 °C under 5% CO_2 in a humidified chamber and passaged upon reaching confluency. For passaging, the cells were treated with cell dissociation buffer (TrypLE; Gibco) for 5 min and subcultured in standard culture medium at 4000 cells/cm^2. Cells at passages 3 (BM-MSCs) and 4 (UC-MSCs, AD-MSCs) were used.

2.2. Cell sheet fabrication

Temperature-responsive cell culture dishes were coated with 1 mL of FBS for 1.5 h before cell seeding of all three MSC types. Specifically, the MSCs were seeded on 35-mm diameter temperature-responsive cell culture dishes (UpCell; CellSeed, Tokyo, Japan) at a density of 2×10^5 cells/dish and cultured until they reached confluency (Fig. 1A). The above-described standard culture medium containing 20% FBS was used for cell sheet fabrication. At day 5, all MSC cultures were harvested as intact monolayer sheets from the culture dishes within 30 min by reducing the temperature to 20 °C. The total cell numbers in the cell sheets were counted by trypan blue exclusion assays using a Vi-Cell XR (Beckman Coulter Inc., Brea, CA, USA) every 24 h after cell seeding.

2.3. Detection of cytokine secretion by enzyme-linked immunosorbent assay (ELISA)

All three types of MSCs were cultured for 5 days to fabricate cell sheets, and the medium was changed to standard cell culture medium (DMEM containing 10% FBS). The cells were incubated for a further 24 h and their supernatants were collected and stored at −80 °C until analysis by ELISA. The cells were then detached and counted by trypan blue exclusion assays. The levels of HGF, IL-6, IL-10, and TGF-β1 in the supernatants from the three types of cell sheets were determined by ELISA kits (Qutantikine ELISA, R&D Systems, Minneapolis, MN, USA) according to the manufacturer's recommendations. The level of PGE_2 in the supernatants was also determined by an ELISA kit (Prostaglandin E2 ELISA kit − monoclonal, Cayman Chemical, Ann Arbor, MI, USA) The cytokine levels were calculated based on a standard curve constructed for each assay. DMEM containing 10% FBS was used as a negative control. The cytokine levels in a negative control were subtracted from each sample value. All samples were run in duplicate at three different times.

2.4. Time-lapse microscopy

The cell adhesion properties of the cell sheets were analyzed by time-lapse microscopy (Fig. 1B). The cell sheets were detached by reducing the culture temperature to 20 °C for 30 min, and then were transferred to 35-mm diameter tissue culture polystyrene (TCPS) dishes (Thermo Fisher Scientific, Waltham, MA, USA) that had been pre-coated with FBS (Gibco) for 1 h prior to cell sheet re-attachment. The cell sheets were incubated for 15 min before images were obtained to allow cell focusing. Images of the cell sheets were taken every 1 min for 6 h using a BZ-9000 microscope (Keyence, Osaka, Japan). The cell sheets were cultured in a thermostated incubation system for the microscope (Tokai Hit, Shizuoka, Japan) while images were acquired.

3. Results and discussion

3.1. Cell adhesion and cell sheet fabrication with UC-MSCs, BM-MSCs, and AD-MSCs

To fabricate cell sheets, UC-MSCs, BM-MSCs, and AD-MSCs were seeded at a density of 2×10^5 cells on temperature-responsive cell culture dishes. The cell morphologies of the three types of MSCs on the culture dishes were observed during cell culture (Fig. 2). All three types of MSCs were cultured for 5 days on the dishes to reach confluency (Fig. 2A1−5, B1−5, C1−5). The cell morphologies of BM-MSCs and UC-MSCs at day 1 differed from that of cells cultured on TCPS dishes regularly used for cell expansion and subculture (Fig. 2A−1, B-1). All cell types were able to be detached as
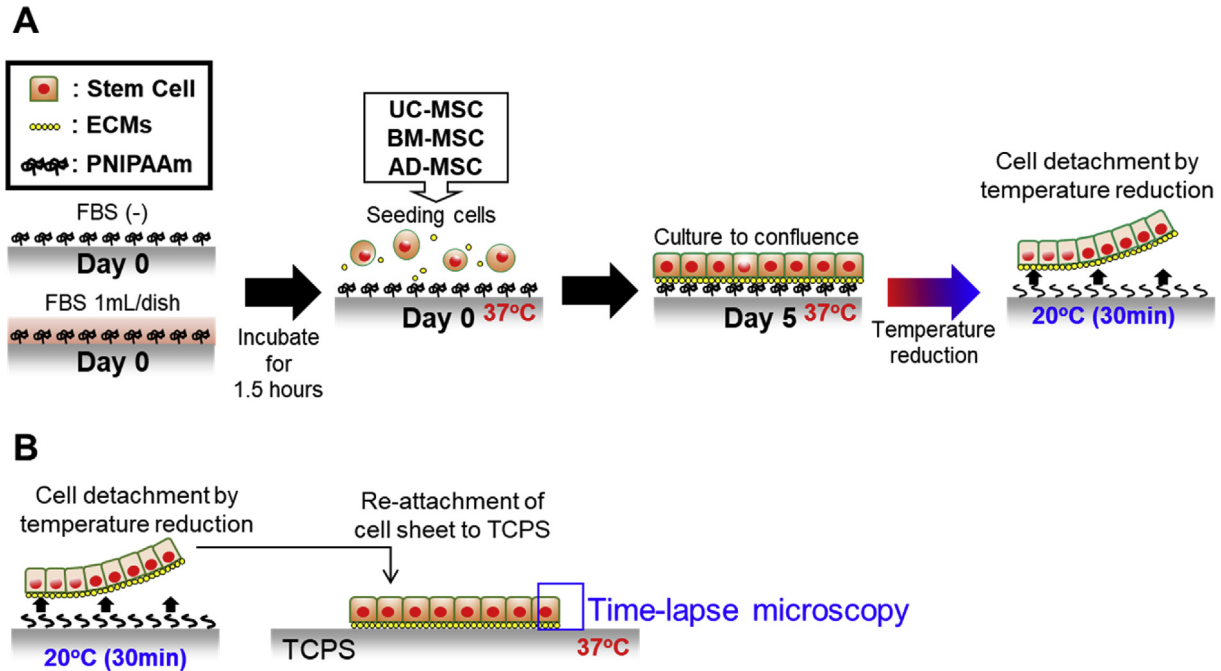
Fig. 1. Illustration of the cell sheet fabrication process. UC-MSCs, BM-MSCs, and AD-MSCs were seeded on 35-mm diameter temperature-responsive cell culture dishes and cultured for 5 days to reach confluency. (A) FBS was pre-coated prior to cell seeding. MSCs were cultured for 5 days to reach confluency, and then harvested from the temperature-responsive cell culture dishes as monolayer cell sheets by reducing the temperature (37 °C–20 °C). (B) The detached cell sheets were transferred to TCPS dishes and incubated for 15 min before observation. Images of cell attachment and cell migration from cell sheets were obtained by time-lapse microscopy.
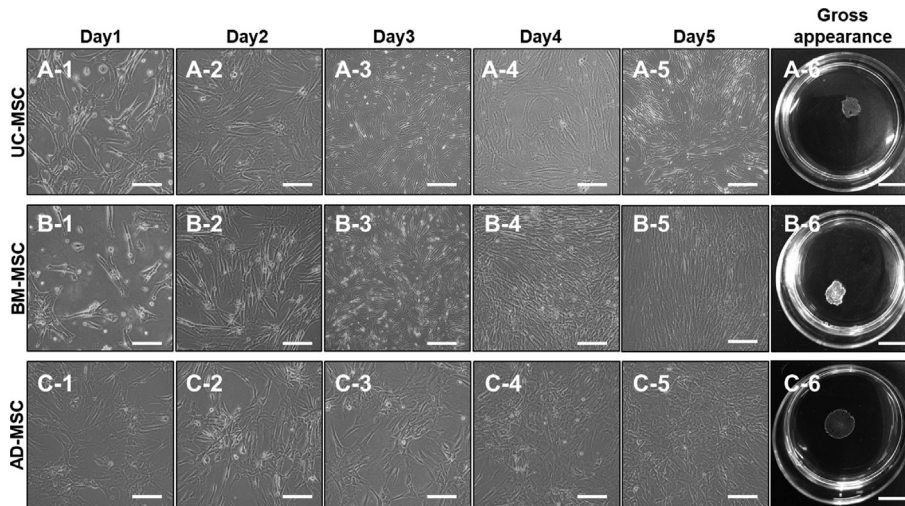

Fig. 2. Fabrication of cell sheets using temperature-responsive cell culture dishes without FBS pre-coating. The morphologies of UC-MSCs, BM-MSCs, and AD-MSC on temperature-responsive cell culture dishes without FBS pre-coating were observed for 5 days after cell seeding. (A–C) The morphologies of UC-MSCs, BM-MSCs, and AD-MSCs were observed by phase-contrast microscopy (A1–5, B1–5, C1–5). The cells were then detached from the temperature-responsive cell culture dishes by reducing the temperature, and gross appearance was observed (A-6, B-6, C-6). Scale bars: 200 μm in A1–5, B1–5, C1–5; 10 mm in 2 A–6, B-6, C-6.

monolayer cell sheets by reducing the temperature to 20 °C for 30 min (Fig. 2A–6, B-6, C-6). UC-MSC, BM-MSC, and AD-MSC sheets gradually became detached from the walls of the temperature-responsive cell culture dishes and shrank (10-mm diameter) upon full detachment from the dishes. This occurred because of the loss of focal adhesion sites between the cell sheets and the cell culture dish surfaces. Furthermore, the retained cell–cell bonds provided cytoskeletal contractile force in the sheets.

To compare fabrication methods for the cell sheets, BM-MSCs, UC-MSCs, and AD-MSCs were seeded on temperature-responsive cell culture dishes that had been pre-coated with FBS for 1.5 h (Fig. 3A1–5, B1–5, C1–5). Cell attachment was enhanced using the FBS-coated dishes. UC-MSCs, BM-MSCs, and AD-MSCs were able to attach and change their morphology from round- to spindle-shaped at day 1. All three types of MSCs were able to be detached as cell sheets using FBS-non-coated temperature-responsive cell culture dishes (Fig. 3A–6, B-6, C-6). BM-MSCs showed lower cell adhesion to the temperature-responsive cell culture dish surfaces than UC-MSCs and AD-MSCs. In fact, the total numbers of BM-MSCs were lower than those of UC-MSCs and AD-MSCs for 48 h after cell seeding. The time for cell sheet detachment showed no significant differences among the cell types for both FBS-non-coated and FBS-
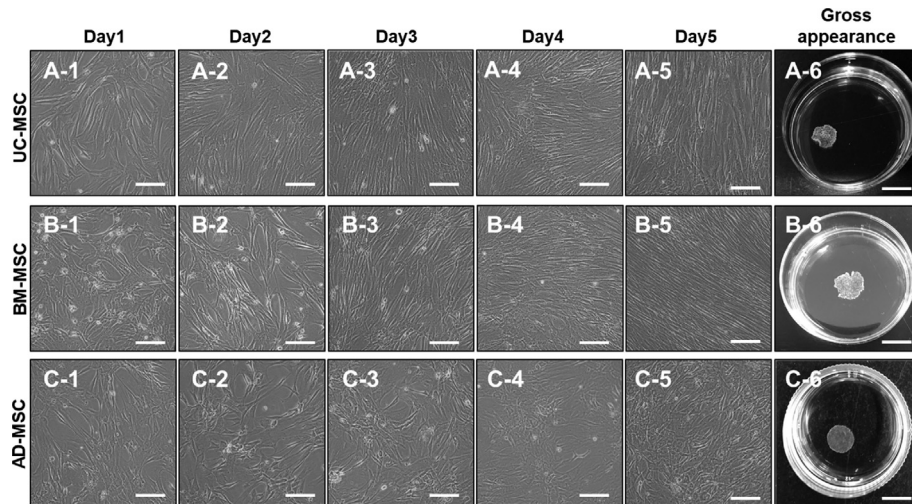
Fig. 3. Fabrication of cell sheets using temperature-responsive cell culture dishes with FBS pre-coating. The morphologies of UC-MSCs, BM-MSCs, and AD-MSCs on temperature-responsive cell culture dishes with FBS pre-coating were observed for 5 days after cell seeding. (A–C) The morphologies of UC-MSCs, BM-MSCs, and AD-MSCs were observed by phase-contrast microscopy (A1–5, B1–5, C1–5). The cells were then detached from the temperature-responsive cell culture dishes by reducing the temperature, and gross appearance was observed (A-6, B-6, C-6). Scale bars: 200 μm in A1–5, B1–5, C1–5; 10 mm in A-6, B-6, C-6.

pre-coated temperature-responsive cell culture dishes. These findings suggest that the adhesion properties were similar among UC-MSCs, BM-MSCs, and AD-MSCs.

The total numbers of cells attached to FBS-pre-coated temperature-responsive cell culture dishes were counted every 24 h after cell seeding for all three cell types. BM-MSCs reached confluency on day 4, while UC-MSCs and AD-MSCs reached confluency on day 5 (Fig. 4A). BM-MSCs showed the highest proliferation rate (6.0×10^5 cells/dish at day 5) compared with UC-MSCs (4.7×10^5 cells/dish at day 5) and AD-MSCs (3.3×10^5 cells/dish at day 5). These findings differ from those in previous studies showing that UC-MSCs had higher proliferation rates than BM-MSCs [55,56]. These differences in proliferation may be related to the passage numbers of the cells and the proliferative ability within the tissues of origin. AD-MSCs had relatively low ability on population doubling compared to BM-MSC and UC-MSC. This is consistent with manufacturer's information, since duration time for subculture of AD-MSCs were 6–7 days.

The total cell numbers of MSCs on day 5 of culture on temperature-responsive cell culture dishes with or without FBS pre-coating were counted by trypan blue exclusion assays (Fig. 4B). The total cell numbers were higher when MSCs were cultured on

FBS-pre-coated dishes. These results suggest that coating of temperature-responsive cell culture dishes with FBS enhanced cell attachment and proliferation in MSC sheets with UC-MSCs and AD-MSCs.

3.2. Cytokine expression in cell sheets fabricated from UC-MSCs, BM-MSCs, and AD-MSCs

The paracrine effect of MSCs involving cytokine secretion is required for long-term stable therapeutic effects. Identification of the cytokines secreted by MSCs is necessary to understand and improve stem cell therapy. To clarify the paracrine effect of cytokines secreted by cell sheets composed of UC-MSCs, BM-MSCs, and AD-MSCs, the protein levels of HGF, TGF-β1, IL-6, IL-10, and PGE$_2$ in supernatants from the cell sheets were analyzed by ELISA (Fig. 5A–E). HGF is known to support cell survival, proliferation, and migration and to suppresses inflammation [57–60]. AD-MSCs showed relatively high levels of HGF secretion, while UC-MSCs produced low levels (Fig. 5A). HGF was also shown to mediate functional recovery of MSCs in animal models of diseases such as multiple sclerosis and COPD [61,62], suggesting that the cell origin
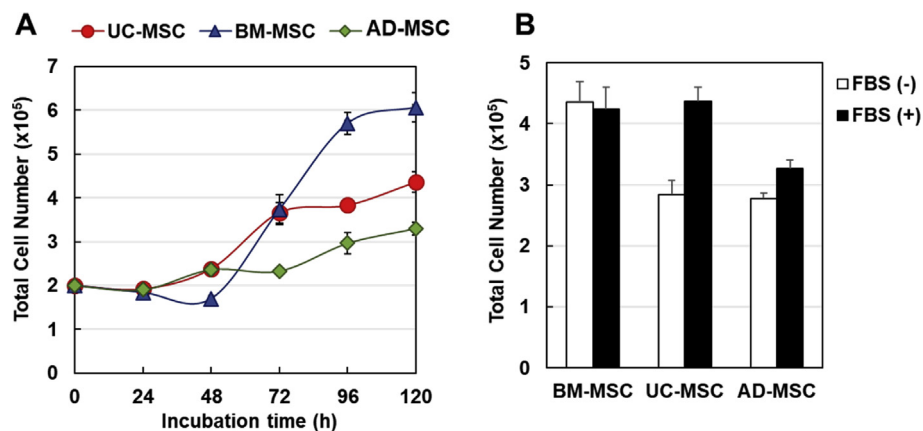

Fig. 4. Proliferative properties of UC-MSCs, BM-MSCs, and AD-MSCs. Total cell numbers were counted by trypan blue exclusion assays. (A) The cell numbers were counted every 24 h during culture on FBS pre-coated temperature-responsive cell culture dishes for 120 h. (B) The total cell numbers of UC-MSCs, BM-MSCs, and AD-MSCs at day 5 were compared between cells cultured with and without FBS pre-coating.
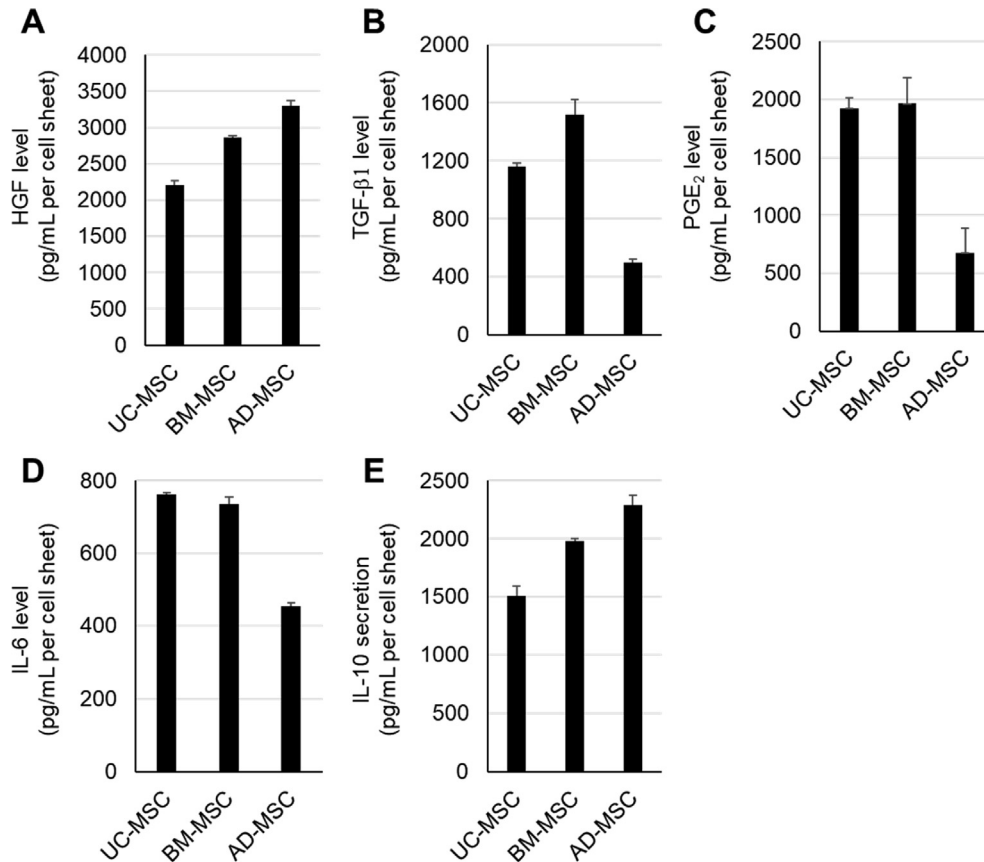
Fig. 5. Comparison of cytokine expression levels from cell sheets composed of UC-MSCs, BM-MSCs, and AD-MSCs. The secreted cytokine levels from UC-MSCs, BM-MSCs, and AD-MSCs were evaluated by ELISA. To determine the cytokine expression levels, the cell culture medium was changed at 24 h prior to sampling. (A–E) The protein levels of HGF (A), TGF-β1 (B), PGE$_2$ (C), IL-6 (D), and IL-10 (E) were measured. Standard culture medium (DMEM containing 10% FBS) was used as a negative control.

of MSCs may affect therapeutic efficacy in some diseases. TGF-β1, PGE$_2$, IL-6, and IL-10 are related to the anti-inflammatory response and immune regulation by MSCs, which is important for cell survival of transplanted MSCs [57]. TGF-β1 down-modulates the inflammatory response by dampening macrophage activity and proinflammatory cytokine secretion [63]. TGF-β1 levels in the supernatants were in the order of BM-MSCs > UC-MSCs > AD-MSCs (Fig. 5B). TGF-β1 exerts pleiotropic effects on processes such as cell proliferation, differentiation, migration, and death [64]. TGF-β1 was also shown to exhibit T cell suppression activity [65], suggesting that the secretion level of TGF-β1 may affect the cell survival of transplanted MSCs. The secretion levels of PGE$_2$ were relatively high in both BM-MSCs and UC-MSCs and decreased in AD-MSCs (Fig. 5C). PGE$_2$ functions in the anti-inflammatory response through binding to its receptors, EP1–EP4 [66]. PGE$_2$ was also reported to enhance the therapeutic effect of MSCs in traumatic brain injury [67], premature ovarian aging [68] suggesting that BM-MSCs and UC-MSCs may show higher therapeutic effects in these conditions. MSC-derived IL-6 was also reported to regulate immune activity and functions as an anti-inflammatory cytokine [69,70]. IL-6 polarizes monocytes toward anti-inflammatory IL-10-producing M2 macrophages [70,71]. IL-10 secreted by MSCs was shown to suppress T cell proliferation [72] and inflammation [73,74]. The anti-inflammatory function of IL-10 occurs through inhibition of Th1 and Th17 cell proliferation and activation and by promoting the development of M2 macrophages [75,76]. IL-6 levels were relatively high in both UC-MSCs and BM-MSCs, while IL-10 levels were relatively high in BM-MSCs and AD-MSCs (Fig. 5D and E),

suggesting BM-MSCs may show higher cell engraftment rates compared with UC-MSCs and AD-MSCs.

All cell types secreted HGF, TGF-β1, PGE$_2$, IL-6, and IL-10, which are important for cell transplantation. Although the cytokine secretion properties differed among the cell types, the required cytokine levels necessary for successful cell transplantation remain to be established.

3.3. Cell adhesion properties of cell sheets

The adhesion properties of the cell sheets were investigated by time-lapse microscopy. Cell sheets composed of UC-MSCs, BM-MSCs, and AD-MSCs were re-attached to TCPS dishes (Fig. 6 and Supplementary Movie). The dishes were also coated with FBS to enhance cell sheet attachment to the TCPS surface. After 15 min of incubation, the cell sheets were gently washed with phosphate-buffered saline to confirm cell attachment to the TCPS surface. Cell sheets fabricated from UC-MSCs, BM-MSCs, and AD-MSCs attached to the TCPS surface within 15 min of incubation. When cells are attached to the surface of a cell culture dish, the cells are stretched and exhibit a spindle shape, while non-attached cells are rounded or cannot be brought into focus using a microscope with a fixed focal lens. Time-lapse microscopy confirmed the cell adhesion of UC-MSC, BM-MSC, and AD-MSC sheets to the TCPS surface. Cells localized to the edges of the UC-MSC, BM-MSC, and AD-MSC sheets were already attached and starting to stretch and migrate (Fig. 6 and Supplementary Movie). The cell attachment and migration
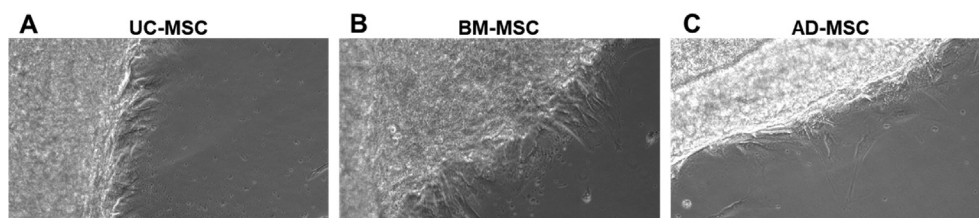
Fig. 6. Cell adhesion property of cell sheets. The cell adhesion properties of cell sheets were analyzed by time-lapse microscopy. (A–C) Cell sheets were placed on TCPS plates and live cell images were obtained by time-lapse microcopy. Cells at the edges of cell sheets were evaluated.

properties were similar among the three cell types, suggesting that their cell attachment rates would be similar upon transplantation. The migration properties may differ over longer periods, because the proliferation rates of UC-MSCs, BM-MSCs, and AD-MSCs were different (Fig. 4A).

These results demonstrate that the three types of MSC sheets would be useful for cell transplantation therapy because of the therapeutic effect of MSCs and the attachment properties of MSC sheets. Because these properties differed slightly among the MSC lines, the MSC sheets should be selected for individual therapeutic applications.

4. Conclusions

In the present study, characterization of cell sheets composed of UC-MSCs, BM-MSCs, and AD-MSCs was performed. Different cell adhesion and proliferation behaviors in temperature-responsive cell culture dishes were observed among the MSC types, probably arising from the cell proliferation abilities within the tissues of origin. Cytokine secretion from the cell sheets was observed. All three types of MSC sheet secreted cytokines with important roles in anti-inflammation, immunosuppression, proliferation, and migration, although slight differences in the secretion of individual cytokines were observed among the different types of cell sheets. The harvested MSC sheets were re-attached on TCPS dishes. The re-attached cell sheets showed rapid adherence to the TCPS surfaces and the cells at the edges of the sheets exhibited migration, suggesting that the fabricated cell sheets retained cellular activity and adhesion ability, which are important for engraftment after cell transplantation. These results demonstrate that MSC sheets can be fabricated from UC-MSCs, BM-MSCs, and AD-MSCs using temperature-responsive cell culture dishes. The MSC sheets could be useful in specific cell transplantation therapies by utilizing appropriate types of MSCs that secrete therapeutic cytokines for the targeted diseases.

Disclosure statement

The authors declare no competing financial interest.

Acknowledgments

Appendix A. Supplementary data

Supplementary data to this article can be found online at https://doi.org/10.1016/j.reth.2019.01.002.

References

[1] Fischbach MA, Bluestone JA, Lim WA. Cell-based therapeutics: the next pillar of medicine. Sci Transl Med 2013;5:179ps7.

[2] Chen Q, Shou P, Zheng C, Jiang M, Cao G, Yang Q, et al. Fate decision of mesenchymal stem cells: adipocytes or osteoblasts? Cell Death Differ 2016;23:1128—39.

[3] Karpov AA, Udalova DV, Pliss MG, Galagudza MM. Can the outcomes of mesenchymal stem cell-based therapy for myocardial infarction be improved? Providing weapons and armour to cells. Cell Prolif 2017;50.

[4] Silva LHA, Antunes MA, Dos Santos CC, Weiss DJ, Cruz FF, Rocco PRM. Strategies to improve the therapeutic effects of mesenchymal stromal cells in respiratory diseases. Stem Cell Res Ther 2018;9:45.

[5] Gnecchi M, Zhang Z, Ni A, Dzau VJ. Paracrine mechanisms in adult stem cell signaling and therapy. Circ Res 2008;103:1204—19.

[6] Figueroa FE, Carrión F, Villanueva S, Khoury M. Mesenchymal Stem Cell treatment for autoimmune diseases:a critical review. Biol Res 2012;45:269—77.

[7] Marquardt LM, Heilshorn SC. Design of injectable materials to improve stem cell transplantation. Curr Stem Cell Rep 2016;2:207—20.

[8] McKee C, Chaudhry GR. Advances and challenges in stem cell culture. Colloids Surfaces B Biointerfaces 2017;159:62—77.

[9] Sekine H, Shimizu T, Dobashi I, Matsuura K, Hagiwara N, Takahashi M, et al. Cardiac cell sheet transplantation improves damaged heart function via superior cell survival in comparison with dissociated cell injection. Tissue Eng A 2011;17:2973—80.

[10] Yamada N, Okano T, Sakai H, Karikusa F, Sawasaki Y, Sakurai Y. Thermoresponsive polymeric surfaces; control of attachment and detachment of cultured cells. Makromol Chem, Rapid Commun 1990;11:571—6.

[11] Takahashi H, Nakayama M, Yamato M, Okano T. Controlled chain length and graft density of thermoresponsive polymer brushes for optimizing cell sheet harvest. Biomacromolecules 2010;11:1991—9.

[12] Mizutani A, Kikuchi A, Yamato M, Kanazawa H, Okano T. Preparation of thermoresponsive polymer brush surfaces and their interaction with cells. Biomaterials 2008;29:2073—81.

[13] Nagase K, Watanabe M, Kikuchi A, Yamato M, Okano T. Thermo-responsive polymer brushes as intelligent biointerfaces: preparation via ATRP and characterization. Macromol Biosci 2011;11:400—9.

[14] Nagase K, Yamato M, Kanazawa H, Okano T. Poly(N-isopropylacrylamide)-based thermoresponsive surfaces provide new types of biomedical applications. Biomaterials 2018;153:27—48.

[15] Nagase K, Okano T, Kanazawa H. Poly(N-isopropylacrylamide) based thermoresponsive polymer brushes for bioseparation, cellular tissue fabrication, and nano actuators. Nano-Structures & Nano-Objects 2018;16:9—23.

[16] Heskins M, Guillet JE. Solution properties of poly(N-isopropylacrylamide). J Macromol Sci A 1968;2:1441—55.

[17] Cammas S, Suzuki K, Sone C, Sakurai Y, Kataoka K, Okano T. Thermoresponsive polymer nanoparticles with a core-shell micelle structure as site-specific drug carriers. J Contr Release 1997;48:157—64.

[18] Akimoto J, Nakayama M, Okano T. Temperature-responsive polymeric micelles for optimizing drug targeting to solid tumors. J Contr Release 2014;193:2—8.

[19] Nakayama M, Akimoto J, Okano T. Polymeric micelles with stimuli-triggering systems for advanced cancer drug targeting. J Drug Target 2014;22:584—99.

[20] Wang J, Ayano E, Maitani Y, Kanazawa H. Enhanced cellular uptake and gene silencing activity of siRNA using temperature-responsive polymer-modified liposome. Int J Pharm 2017;523:217—28.

[21] Mori T, Maeda M. Temperature-responsive formation of colloidal nanoparticles from poly(N-isopropylacrylamide) grafted with single-stranded DNA. Langmuir 2003;20:313—9.

[22] Lai JJ, Hoffman JM, Ebara M, Hoffman AS, Estournès C, Wattiaux A, et al. Dual magnetic-/temperature-responsive nanoparticles for microfluidic separations and assays. Langmuir 2007;23:7385—91.

[23] Hoffman JM, Ebara M, Lai JJ, Hoffman AS, Folch A, Stayton PS. A helical flow, circular microreactor for separating and enriching "smart" polymer-antibody capture reagents. Lab Chip 2010;10:3130—8.

[24] Matsuura M, Ohshima M, Hiruta Y, Nishimura T, Nagase K, Kanazawa H. LAT1-Targeting thermoresponsive fluorescent polymer probes for cancer cell imaging. Int J Mol Sci 2018;19:1646.

[25] Kanazawa H, Yamamoto K, Matsushima Y, Takai N, Kikuchi A, Sakurai Y, et al. Temperature-responsive chromatography using poly(*N*-iso-propylacrylamide)-Modified silica. Anal Chem 1996;68:100—5.

[26] Nagase K, Kobayashi J, Okano T. Temperature-responsive intelligent interfaces for biomolecular separation and cell sheet engineering. J R Soc Interface 2009;6:S293—309.

[27] Nagase K, Hatakeyama Y, Shimizu T, Matsuura K, Yamato M, Takeda N, et al. Thermoresponsive cationic copolymer brushes for mesenchymal stem cell separation. Biomacromolecules 2015;16:532—40.

[28] Nagase K, Okano T. Thermoresponsive-polymer-based materials for temperature-modulated bioanalysis and bioseparations. J Mater Chem B 2016;4:6381—97.

[29] Nagase K, Shukuwa R, Onuma T, Yamato M, Takeda N, Okano T. Micro/nano-imprinted substrates grafted with a thermoresponsive polymer for thermally modulated cell separation. J Mater Chem B 2017;5:5924—30.

[30] Nagase K, Sakurada Y, Onizuka S, Iwata T, Yamato M, Takeda N, et al. Thermoresponsive polymer-modified microfibers for cell separations. Acta Biomater 2017;53:81—92.

[31] Ebara M, Yamato M, Nagai S, Aoyagi T, Kikuchi A, Sakai K, et al. Incorporation of new carboxylate functionalized co-monomers to temperature-responsive polymer-grafted cell culture surfaces. Surf Sci 2004;570:134—41.

[32] Ebara M, Yamato M, Aoyagi T, Kikuchi A, Sakai K, Okano T. Temperature-responsive cell culture surfaces enable "On-Off" affinity control between cell integrins and RGDS ligands. Biomacromolecules 2004;5:505—10.

[33] Arisaka Y, Kobayashi J, Ohashi K, Tatsumi K, Kim K, Akiyama Y, et al. A heparin-modified thermoresponsive surface with heparin-binding epidermal growth factor-like growth factor for maintaining hepatic functions in vitro and harvesting hepatocyte sheets. Regenerative Therapy 2016;3:97—106.

[34] Arisaka Y, Kobayashi J, Yamato M, Akiyama Y, Okano T. Switching of cell growth/detachment on heparin-functionalized thermoresponsive surface for rapid cell sheet fabrication and manipulation. Biomaterials 2013;34:4214—22.

[35] Okano T, Yamada N, Okuhara M, Sakai H, Sakurai Y. Mechanism of cell detachment from temperature-modulated, hydrophilic-hydrophobic polymer surfaces. Biomaterials 1995;16:297—303.

[36] Okano T, Kikuchi A, Sakurai Y, Takei Y, Ogata N. Temperature-responsive poly(N-isopropylacrylamide) as a modulator for alteration of hydrophilic/hydrophobic surface properties to control activation/inactivation of platelets. J Contr Release 1995;36:125—33.

[37] Yamato M, Okuhara M, Karikusa F, Kikuchi A, Sakurai Y, Okano T. Signal transduction and cytoskeletal reorganization are required for cell detachment from cell culture surfaces grafted with a temperature-responsive polymer. J Biomed Mater Res 1999;44:44—52.

[38] Kushida A, Yamato M, Konno C, Kikuchi A, Sakurai Y, Okano T. Decrease in culture temperature releases monolayer endothelial cell sheets together with deposited fibronectin matrix from temperature-responsive culture surfaces. J Biomed Mater Res 1999;45:355—62.

[39] Kushida A, Yamato M, Kikuchi A, Okano T. Two-dimensional manipulation of differentiated Madin-Darby canine kidney (MDCK) cell sheets: the noninvasive harvest from temperature-responsive culture dishes and transfer to other surfaces. J Biomed Mater Res 2001;54:37—46.

[40] Nishida K, Yamato M, Hayashida Y, Watanabe K, Yamamoto K, Adachi E, et al. Corneal reconstruction with tissue-engineered cell sheets composed of autologous oral mucosal epithelium. N Engl J Med 2004;351:1187—96.

[41] Sawa Y, Miyagawa S, Sakaguchi T, Fujita T, Matsuyama A, Saito A, et al. Tissue engineered myoblast sheets improved cardiac function sufficiently to discontinue LVAS in a patient with DCM: report of a case. Surg Today 2012;42:181—4.

[42] Ohki T, Yamato M, Ota M, Takagi R, Murakami D, Kondo M, et al. Prevention of esophageal stricture after endoscopic submucosal dissection using tissue-engineered cell sheets. Gastroenterology 2012;143. 582-588.e2.

[43] Iwata T, Yamato M, Tsuchioka H, Takagi R, Mukobata S, Washio K, et al. Periodontal regeneration with multi-layered periodontal ligament-derived cell sheets in a canine model. Biomaterials 2009;30:2716—23.

[44] Kanzaki M, Yamato M, Yang J, Sekine H, Kohno C, Takagi R, et al. Dynamic sealing of lung air leaks by the transplantation of tissue engineered cell sheets. Biomaterials 2007;28:4294—302.

[45] Ebihara G, Sato M, Yamato M, Mitani G, Kutsuna T, Nagai T, et al. Cartilage repair in transplanted scaffold-free chondrocyte sheets using a minipig model. Biomaterials 2012;33:3846—51.

[46] Yamamoto K, Yamato M, Morino T, Sugiyama H, Takagi R, Yaguchi Y, et al. Middle ear mucosal regeneration by tissue-engineered cell sheet transplantation. npj Regenerative Medicine 2017;2:6.

[47] Masuda S, Matsuura K, Anazawa M, Iwamiya T, Shimizu T, Okano T. Formation of vascular network structures within cardiac cell sheets from mouse embryonic stem cells. Regenerative Therapy 2015;2:6—16.

[48] Iwata T, Yamato M, Washio K, Yoshida T, Tsumanuma Y, Yamada A, et al. Periodontal regeneration with autologous periodontal ligament-derived cell sheets — a safety and efficacy study in ten patients. Regenerative Therapy 2018;9:38—44.

[49] Fujita I, Utoh R, Yamamoto M, Okano T, Yamato M. The liver surface as a favorable site for islet cell sheet transplantation in type 1 diabetes model mice. Regenerative Therapy 2018;8:65—72.

[50] Kato Y, Iwata T, Morikawa S, Yamato M, Okano T, Uchigata Y. Allogeneic transplantation of an adipose-derived stem cell sheet combined with artificial skin accelerates wound healing in a rat wound model of type 2 diabetes and obesity. Diabetes 2015;64:2723—34.

[51] Kaibuchi N, Iwata T, Yamato M, Okano T, Ando T. Multipotent mesenchymal stromal cell sheet therapy for bisphosphonate-related osteonecrosis of the jaw in a rat model. Acta Biomater 2016;42:400—10.

[52] Nagase K, Nagumo Y, Kim M, Kim H-J, Kyung H-W, Chung H-J, et al. Local release of VEGF using fiber mats enables effective transplantation of layered cardiomyocyte sheets. Macromol Biosci 2017;17:1700073.

[53] Maruya Y, Kanai N, Kobayashi S, Koshino K, Okano T, Eguchi S, et al. Autologous adipose-derived stem cell sheets enhance the strength of intestinal anastomosis. Regenerative Therapy 2017;7:24—33.

[54] Hamada M, Iwata T, Kato Y, Washio K, Morikawa S, Sakurai H, et al. Xenogeneic transplantation of human adipose-derived stem cell sheets accelerate angiogenesis and the healing of skin wounds in a Zucker Diabetic Fatty rat model of obese diabetes. Regenerative Therapy 2017;6:65—73.

[55] Hass R, Kasper C, Böhm S, Jacobs R. Different populations and sources of human mesenchymal stem cells (MSC)- A comparison of adult and neonatal tissue-derived MSC. Cell Commun Signal 2011;9.

[56] Lu L-L, Liu Y-J, Yang S-G, Zhao Q-J, Wang X, Gong W, et al. Isolation and characterization of human umbilical cord mesenchymal stem cells with hematopoiesis-supportive function and other potentials. Haematologica 2006;91:1017—26.

[57] Madrigal M, Rao KS, Riordan NH. A review of therapeutic effects of mesenchymal stem cell secretions and induction of secretory modification by different culture methods. J Transl Med 2014;12.

[58] Benkhoucha M, Santiago-Raber ML, Schneiter G, Chofflon M, Funakoshi H, Nakamura T, et al. Hepatocyte growth factor inhibits CNS autoimmunity by inducing tolerogenic dendritic cells and CD25+Foxp3+ regulatory T cells. Proc Natl Acad Sci U S A 2010;107:6424—9.

[59] Ito W, Kanehiro A, Matsumoto K, Hirano A, Ono K, Maruyama H, et al. Hepatocyte growth factor attenuates airway hyperresponsiveness, inflammation, and remodeling. Am J Respir Cell Mol Biol 2005;32:268—80.

[60] Rutella S, Bonanno G, Procoli A, Mariotti A, de Ritis DG, Curti A, et al. Hepatocyte growth factor favors monocyte differentiation into regulatory interleukin (IL)-10++IL-12low/neg accessory cells with dendritic-cell features. Blood 2006;108:218—27.

[61] Bai L, Lennon DP, Caplan AI, DeChant A, Hecker J, Kranso J, et al. Hepatocyte growth factor mediates mesenchymal stem cell-induced recovery in multiple sclerosis models. Nat Neurosci 2012;15:862—70.

[62] Kennelly H, Mahon BP, English K. Human mesenchymal stromal cells exert HGF dependent cytoprotective effects in a human relevant pre-clinical model of COPD. Sci Rep 2016;6:38207.

[63] Wahla SM, Orensteinb JM, Chen W. TGF-β influences the life and death decisions of T lymphocytes. Cytokine Growth Factor Rev 2000;11:71—9.

[64] Oshimori N, Fuchs E. The harmonies played by TGF-beta in stem cell biology. Cell Stem Cell 2012;11:751—64.

[65] Niu J, Yue W, Le-Le Z, Bin L, Hu X. Mesenchymal stem cells inhibit T cell activation by releasing TGF-β1 from TGF-β1:GARP complex. Oncotarget 2017;8:99784—800.

[66] Gomez I, Foudi N, Longrois D, Norel X. The role of prostaglandin E2 in human vascular inflammation. Prostagl Leukot Essent Fat Acids 2013;89:55—63.

[67] Kota DJ, Prabhakara KS, Toledano-Furman N, Bhattarai D, Chen Q, DiCarlo B, et al. Prostaglandin E2 indicates therapeutic efficacy of mesenchymal stem cells in experimental traumatic brain injury. Stem Cell 2017;35:1416—30.

[68] Ding C, Li H, Wang Y, Wang F, Wu H, Chen R, et al. Different therapeutic effects of cells derived from human amniotic membrane on premature ovarian aging depend on distinct cellular biological characteristics. Stem Cell Res Ther 2017;8:173.

[69] Li P, Li SH, Wu J, Zang WF, Dhingra S, Sun L, et al. Interleukin-6 down-regulation with mesenchymal stem cell differentiation results in loss of immunoprivilege. J Cell Mol Med 2013;17:1136—45.

[70] Bernardo ME, Fibbe WE. Mesenchymal stromal cells: sensors and switchers of inflammation. Cell Stem Cell 2013;13:392—402.

[71] Eggenhofer E, Hoogduijn MJ. Mesenchymal stem cell-educated macrophages. Transplant Res 2012;1.

[72] Yang SH, Park MJ, Yoon IH, Kim SY, Hong SH, Shin JY, et al. Soluble mediators from mesenchymal stem cells suppress T cell proliferation by inducing IL-10. Exp Mol Med 2009;41:315—24.

[73] Duffy MM, Ritter T, Ceredig R, Griffin MD. Mesenchymal stem cell effects on T-cell effector pathways. Stem Cell Res Ther 2011;2.

[74] Choi JJ, Yoo SA, Park SJ, Kang YJ, Kim WU, Oh H, et al. Mesenchymal stem cells overexpressing interleukin-10 attenuate collagen-induced arthritis in mice. Clin Exp Immunol 2008;153:269—76.

[75] Deng B, Wehling-Henricks M, Villalta SA, Wang Y, Tidball JG. IL-10 triggers changes in macrophage phenotype that promote muscle growth and regeneration. J Immunol 2012;189:3669—80.

[76] Gu Y, Yang J, Ouyang X, Liu W, Li H, Yang J, et al. Interleukin 10 suppresses Th17 cytokines secreted by macrophages and T cells. Eur J Immunol 2008;38:1807—13.